

## Overview of the research activities and results at Puijo semi-urban measurement station

Ari Leskinen<sup>1)</sup>, Harri Portin<sup>1)</sup>, Mika Komppula<sup>1)</sup>, Pasi Miettinen<sup>2)</sup>, Antti Arola<sup>1)</sup>, Heikki Lihavainen<sup>3)</sup>, Juha Hatakka<sup>3)</sup>, Ari Laaksonen<sup>2)3)</sup> and Kari E. J. Lehtinen<sup>1)2)</sup>

<sup>1)</sup> Finnish Meteorological Institute, Kuopio Unit, P.O. Box 1627, FI-70211 Kuopio, Finland

<sup>2)</sup> Department of Physics, University of Kuopio, P.O. Box 1627, FI-70211 Kuopio, Finland

<sup>3)</sup> Finnish Meteorological Institute, Research and Development, P.O. Box 503, FI-00101 Helsinki, Finland

Received 12 Dec. 2008, accepted 11 Mar. 2009 (Editor in charge of this article: Veli-Matti Kerminen)

Leskinen, A., Portin, H., Komppula, M., Miettinen, P., Arola, A., Lihavainen, H., Hatakka, J., Laaksonen, A. & Lehtinen, K. E. J. 2009: Overview of the research activities and results at Puijo semi-urban measurement station. *Boreal Env. Res.* 14: 576–590.

We introduce a new measurement station that we established in 2005 in an observation tower at Puijo in Kuopio. At Puijo we measure several meteorological parameters, aerosol and cloud droplet size distribution, aerosol optical properties and trace gas concentrations. We summarize the research activities at the station during its three-year history and present overall results. We compare the results from Puijo with those measured at the ground level in Kuopio and at the Finnish background stations. We also characterize the measured parameters according to the wind direction and air mass origins, based on trajectory analysis, for the effects of local and remote sources. Our conclusion is that the Puijo tower is a very good place to gather experimental data on cloud formation and aerosol–cloud interaction. In addition to cloud experiments, we would suggest the Puijo measurement station for studies of particle formation, which we also observed frequently.

## Introduction

Atmospheric fine particles affect the climate directly by scattering and absorbing energy, and indirectly through cloud formation and cloud optical properties. The effect of aerosols on the climate is cooling but it still possesses a great uncertainty (IPCC 2007). In order to reduce this uncertainty, we need better climatic model estimations, and in order to develop these climatic models, we need more experimental data.

One important factor in model estimations are the aerosol–cloud interactions, especially activation of the fine particles into cloud drop-

lets. One can study these phenomena by carrying out aircraft measurements in clouds. Aircraft measurements are, however, short-term, complex, and expensive, and they require instruments with very fast time resolution.

For long-term measurements, one would prefer stationary, ground-based measurement at locations, which are at times surrounded by clouds. These kinds of locations are, for example, the GAW (Global Atmospheric Watch) stations at Pallas in Finland (Hatakka *et al.* 2003) and at Jungfraujoch in Switzerland (Baltensperger *et al.* 1997). In 2005, we started similar particle and cloud research in Kuopio, Finland, on the top

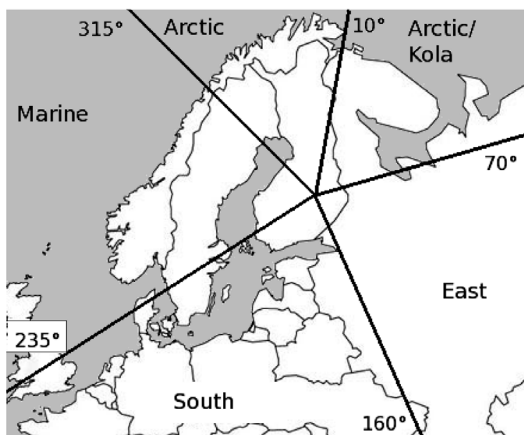


**Fig. 1.** Location of Puijo measurement site in Kuopio, Finland. The lines define five sectors for trajectory calculations: Arctic ( $315^{\circ}$ – $10^{\circ}$ ), Arctic/Kola ( $10^{\circ}$ – $70^{\circ}$ ), East ( $70^{\circ}$ – $160^{\circ}$ ), South ( $160^{\circ}$ – $235^{\circ}$ ) and Marine ( $235^{\circ}$ – $315^{\circ}$ ). The marine areas are in grey.

of an observation tower at Puijo. Our measurements at Puijo produce data from a semi-urban environment for aerosol–cloud interaction studies as well as for particle formation studies.

In this paper, we introduce the Puijo measurement station and summarize the activities and overall results gathered during its three-year history. We also compare the data from Puijo with those measured at the ground level in Kuopio and at Finnish background and boreal forest stations.

## Material and methods

### Experimental sites

Kuopio (population 91 000) is the principal town of the province of Northern Savo, in the eastern part of central Finland, 330 km northeast from Helsinki, the capital of Finland (Fig. 1). The town is located on a peninsula surrounded by Lake Kallavesi 82 m a.s.l. (Fig. 2).

The main part of the district of Northern Savo, and especially the neighbourhood of Kuopio, belongs to the southern boreal climatic zone and is characterized by forests with conifer (mostly pine and spruce) and deciduous (mostly birch) trees, an undulating terrain with rocky soil and moderate height hills, and lots of long lakes in the northwest–southeast direction. The



**Fig. 2.** Surroundings of Puijo measurement site. 1 = Puijo observation tower, 2 = Savilahti automatic weather station, 3 = district heating plant, 4 = pulp mill, 5 = highway. The lake is in grey.

vast lake district acts as a heat storage and increases the nightly temperatures in summers, thus lengthening the growing period.

The most significant local sources are traffic on highways (national/European highway 5/E63 and national highway 17), especially between Kuopio and Siilinjärvi with approximately 30 000 vehicles/day, the local traffic in Kuopio, and point sources, such as a district heating plant 3 km south of Puijo and a pulp mill 5 km northeast of Puijo (Fig. 2).

The nearest towns are Siilinjärvi (20 000 inhabitants, 20 km north of Kuopio), Varkaus (23 000 inhabitants, 70 km south of Kuopio), Iisalmi (22 000 inhabitants, 80 km north of Kuopio), Joensuu (57 000 inhabitants, 110 km east of Kuopio), and Jyväskylä (85 000 inhabitants, 120 km southwest of Kuopio).

### Puijo ( $62^{\circ}54'32''N$ , $27^{\circ}39'31''E$ )

The Puijo measurement station is on the top of an observation tower, 306 m a.s.l. and 224 m above the surrounding lake level. The tower is

**Table 1.** Summary of permanent measurements at the Pujo measurement site.

Component	Measurement method/instrument	Period
Aerosol light absorbing coefficient	Multi-angle absorption photometer (Thermo MAAP 5012)	Aug 2006–
Aerosol number concentration	Condensation particle counter (TSI 3010 CPC, 3785 WCPC)	Jun 2006–
Aerosol light scattering coefficient	Three wavelength integrating nephelometer (TSI 3563)	Aug 2006–
Aerosol size distribution (cloud interstitial)	Differential mobility particle sizer (DMPS, 7–800 nm)	Jun 2006–
Aerosol size distribution (total)	DMPS (7–800 nm), dust monitor (Grimm #190, 0.25–32 µm)	Jun 2006–
Aerosol optical pressure sensor (Vaisala BAROCAP®)	Capacitive absolute pressure sensor (Vaisala BAROCAP®)	Oct 2005–
Cloud droplet size distribution	Optical cloud droplet spectrometer (DMT, 2–50 µm)	Aug 2006–
Icing conditions	Ice detector (ICEMET)	Nov 2007–Aug 2008
Nitrogen oxide concentration	Chemiluminescent NO-NO <sub>x</sub> analyzer (Thermo 42i)	Oct 2006
Ozone concentration	UV photometric O <sub>3</sub> analyzer (Thermo 49i)	Oct 2006–
Sulphur dioxide concentration	UV fluorescence SO <sub>2</sub> analyzer (Thermo 43-TLE)	Oct 2006–
Temperature and relative humidity	Pt100 and Vaisala HUMICAP®	Oct 2005–
Temperature and relative humidity	Vaisala HMT330MIK	Jun 2008–
Visibility, present weather and precipitation	Present weather sensor (Vaisala FD12P)	Oct 2005–
Weather (visually)	Weather camera and camera server (Axis 247S)	Jun 2008–
Wind speed and direction	Ultrasonic two-dimensional anemometer (Thies UA2D)	Oct 2005–

a 75 m high building on the Pujo hill, approximately 2 km northwest of the center of Kuopio (Fig. 2).

Our research groups at the Finnish Meteorological Institute (FMI) in Kuopio and Helsinki and at the University of Kuopio established the station in 2005. We instrumented the station for continuous measurements of aerosols, cloud droplets, weather parameters and trace gases (Table 1). We started measuring the weather parameters on 12 October 2005, the aerosol size distribution and total number concentration on 1 June 2006, aerosol optical properties (light absorbing and scattering coefficient) on 26 August 2006, and concentrations of trace gases on 30 October 2006.

In addition to the permanent measurements at Pujo, we organized there three intensive measurement campaigns with an extended set of instruments in 2006–2008. We used an aerosol mass spectrometer for aerosol chemical composition studies, a cloud condensation nuclei counter for cloud droplet activation studies and different tandem differential mobility analyzers for aerosol hygroscopicity and organic compound affinity studies. We arranged the first aerosol–cloud experiment (PuCE1) between 16 October and 17 November 2006, the second (PuCE2) between 24 August and 24 September 2007, and the third (PuCE3) between 17 September and 16 October 2008. The third campaign was also one of the EUCAARI/EMEP (European Integrated project on Aerosol Cloud Climate and Air Quality Interactions/European Monitoring and Evaluation Programme) intensive measurement campaigns in 2008. Since we intend this paper to be an overview of the activities at Pujo and since the data from the measurement campaigns are extensive, we will handle them in separate forthcoming papers.

#### Savilahti (62°53'32''N, 27°38'12''E)

The Savilahti station is an automatic weather station (AWS) at the University of Kuopio 2 km southwest of Pujo, 87 m a.s.l. (Fig. 2). The Kuopio Savilahti AWS belongs to the FMI weather observation network and is used for automatic weather observation including also

solar irradiation and flux measurements (Table 2). The AWS collects data every 10 minutes and the measurements at Savilahti have been continuous since June 2005.

## Experimental setup at Puijo

## Sampling lines

At Puijo we draw the samples to the instruments through two parallel sampling lines, one with a PM10 inlet followed by a PM2.5 cyclone (interstitial inlet), and the other with a heated inlet and heated snow-hood in order to dry the cloud droplets (total air inlet). The length and diameter are 7.4 m and 33 mm for the interstitial particle sampling line and 6.1 m and 60 mm for the total air sampling line, respectively. The target flow rates through these lines are  $16.7 \text{ l min}^{-1}$  and  $50 \text{ l min}^{-1}$ , respectively. The total air inlet has the same construction as that used and designed by Weingartner *et al.* (1999). The cut-off size of the inlet is  $40 \mu\text{m}$  when the wind speed is below  $20 \text{ m s}^{-1}$ . Our calculations of the typical wind speed at Puijo during cloud events (maximum  $16 \text{ m s}^{-1}$ ) indicate that the sampling efficiency of the total inlet system is well above 95% in the size range of  $10\text{--}40 \mu\text{m}$ , which is relevant for aerosol–cloud interaction studies.

We determined the particle losses in the transport lines both by measuring them directly and by calculating them by using a theoretical approach. We measured the particle losses for 0.03–0.2  $\mu\text{m}$  sized NaCl particles and 0.6 and 1.36  $\mu\text{m}$  sized polystyrene latex (PSL) particles, and found that the particle losses in the sampling lines are size-dependent. The losses were largest for 0.03  $\mu\text{m}$  particles, being 27% and 20% for the interstitial particle and the total air sampling lines, respectively. We take the particle losses into account when we invert the particle size distribution for each sampling line from the raw data.

## Meteorological parameters

The instruments for measurement of the meteorological parameters are located on the top roof

**Table 2** Summary of permanent measurements at the Saviljati automatic weather station

Component	Measurement method/instrument	Period
Aerosol optical depth (and other aerosol optical properties)	Sunphotometer (Cimel 318A)	Apr 2008–Jun 2005–
Atmospheric pressure	Capacitive absolute pressure sensor (Vaisala PTB201A)	Jun 2005–
Cloud base height	Ceilometer (Vaisala CT25K)	Jun 2005–
Rainfall	Raingauge with weighing (OTT Pluvio)	Jun 2005–
Snow depth	Snow depth sensor (Campbell Scientific SR50-45)	Dec 2005–
Solar flux	Pyranometer (Kipp & Zonen CMP-21)	Jun 2008–
Sunshine duration	Sunshine duration sensor (Siggeklow SONI)	Jun 2005–
Temperature and relative humidity	Pentronic Pt100 and Vaisala HMP45D	Jun 2005–
Visibility, present weather and precipitation	Present weather sensor (Vaisala FD12P)	Jun 2005–
Wind speed and direction	Ultrasonic two-dimensional anemometer (Thies UA2D)	Jun 2005–

of the Puijo observation tower. The temperature and relative humidity transmitter (Vaisala HMT337) is included in the Meteorological Installation Kit (Vaisala HMT330 MIK) which we installed to a vertical mast on the rooftop at a 2-m height in June 2008. Before this, since October 2005, we had measured the temperature and relative humidity at the same height with a different setup (Pt100 and Vaisala HUMICAP). We also measure the atmospheric pressure with a capacitive absolute pressure sensor (Vaisala BAROCAP) and the horizontal wind speed and direction with an ultrasonic two-dimensional anemometer (Thies UA2D). The anemometer is attached to a horizontal 1-m pole attached to the vertical mast at a 5-m height in order to minimize the effect of turbulence caused by the tower and the antennas on the roof. We also use a present weather sensor (Vaisala FD12P) to characterize the prevailing weather, including visibility and precipitation intensity and type.

#### Nitric oxide, nitrogen dioxide, ozone and sulphur dioxide concentrations

We measure the concentrations of nitric oxide (NO) and nitrogen dioxide ( $\text{NO}_2$ ) at the Puijo station, as they play an important role in the photochemical processes by using a chemiluminescent  $\text{NO}-\text{NO}_x$  analyzer (Thermo Inc., Model 42i). In the analyzer, NO and ozone ( $\text{O}_3$ ) molecules react with each other to produce a characteristic luminescence, whose intensity is linearly proportional to the NO concentration. The analyzer measures the NO concentration directly, and the summed concentration of NO and  $\text{NO}_2$  (denoted as  $\text{NO}_x$ ) by leading the sample through a reducing molybdenum  $\text{NO}_2$ -to-NO converter unit, and then calculates the  $\text{NO}_2$  concentration by subtracting the measured NO concentration from the measured  $\text{NO}_x$  concentration. The analyzer at Puijo operates in the concentration range of 0.05–200 ppb.

For ozone concentration measurements we use an analyzer (Thermo Inc., Model 49i) which is based on the principle that  $\text{O}_3$  molecules absorb UV light at a wavelength of 254 nm. This UV light absorption is directly related to the  $\text{O}_3$  concentration. The  $\text{O}_3$  analyzer at Puijo covers a concentration range of 1–500 ppb.

Our sulphur dioxide analyzer (Thermo Inc., Model 43i-TLE) uses the principle that a molecule ( $\text{SO}_2$ ) absorbs UV light at one wavelength, becoming excited, which then decays to a lower energy state, emitting UV light at a different wavelength. The intensity of the emitted light is proportional to the  $\text{SO}_2$  concentration. At Puijo, we measure the  $\text{SO}_2$  concentration in the range of 0.1–100 ppb.

In all gas analyzers we use a sample flow rate of  $0.5 \text{ l min}^{-1}$  and a time interval of 10 s in data acquisition, and collect the data with self-made measurement programs. We calibrate the analyzers two times a year and take into account the drift in the zero level and the span by correcting the data afterwards with a linear interpolation between consecutive calibration points. The observed drift in the zero level so far has been  $(0.01 \pm 0.41)$  ppb,  $(0.01 \pm 0.13)$  ppb, and  $(0.03 \pm 0.03)$  ppb for  $\text{NO}-\text{NO}_x$  analyzer,  $\text{O}_3$  analyzer, and  $\text{SO}_2$  analyzer, respectively. The gas concentration measurements at Puijo have been running continuously since October 2006.

#### Aerosol size distribution and number concentration

We measure the total number concentration of particles from the total air sampling line with a condensation particle counter (TSI Model 3010 CPC) and the aerosol size distribution from both the interstitial particle and the total air sampling line with a differential mobility particle sizer (DMPS). Until 30 March 2007, we had measured the size distribution in the size range of 10–500 nm until we installed a twin DMPS system on 3 April 2007 to cover the size range of 7–800 nm. We also measure the size distribution of accumulation and coarse mode particles by using an aerosol dust monitor (Grimm Model #190 ADM) in the particle size range of 0.25–32  $\mu\text{m}$ . The twin DMPS consists of two differential mobility analyzer (DMA) tubes, one 11-cm long (denoted as short tube hereafter) and the other 28-cm long (denoted as long tube hereafter), and a condensation particle counter (TSI Model 3010 CPC) after each DMA tube. In both DMPS systems, a beta radiation source ( $\text{Ni-63}$ , 10 mCi = 370 MBq) before the DMA neutralizes the sample into a

charge equilibrium (Wiedensohler 1988). Both DMPS systems have a closed loop sheath flow arrangement with a silica dryer and temperature and humidity sensors. The sheath air flow is 14.2 l min<sup>-1</sup> in the short and 5.6 l min<sup>-1</sup> in the long tube. The aerosol inlet flow is 2.0 l min<sup>-1</sup> in the short and 1.0 l min<sup>-1</sup> in the long tube. The measured size ranges are 7–49 nm with 17 discrete bins for the short tube and 27–800 nm with 29 discrete bins for the long tube. We use the measurements in the overlapping size range of 27–49 nm with 6 discrete bins to adjust the data from each tube to match in the overlapping region.

We measure both the interstitial and the total aerosol size distributions with the same DMPS systems by using a synchronized valve system in two 6-min cycles. During the first cycle the short tube measures the total particle size distribution and the long tube the interstitial particle size distribution, whereas during the second cycle the short tube measures the interstitial particle size distribution and the long tube the total particle size distribution. By using this method we are able to get the entire particle size distribution (7–800 nm) from both sampling lines every 12 min.

### Aerosol optical properties

We measure aerosol extinction coefficients, i.e. light scattering and absorption coefficient with an integrating nephelometer (TSI Model 3563) and a multi-angle absorption photometer (Thermo Model 5012 MAAP), respectively.

The nephelometer measures the scattering and backscattering coefficients at three wavelengths (450 nm for “blue” light, 550 nm for “green” light, and 700 nm for “red” light) by illuminating the sample volume from the side and detecting the light scattered by aerosol particles and gas molecules with a photomultiplier tube over an angle of 7°–170°. The flow rate through the nephelometer is approximately 10 l min<sup>-1</sup>. The nephelometer is calibrated every three months with pure carbon dioxide and filtered air.

The MAAP (Petzold and Schönlinner 2004) determines aerosol light absorption by illuminating a particle-loaded filter with light and measuring simultaneously the radiation passing through the filter. It also measures the light scattered

from the filter at several detection angles in order to resolve the influence of aerosol components that scatter light on the back-scattered radiation. This compensation of light-scattering effects improves considerably the aerosol absorption measurement in filter-based appliances. The flow rate through our MAAP is 5 l min<sup>-1</sup>.

### Cloud droplet size distribution and number concentration

We measure cloud droplet size distribution with a cloud droplet probe (CDP) and particle analysis and collection software (PACS) by Droplet Measurement Technologies. Our CDP has a special inlet system for ground-based measurements, which consists of an inlet nozzle through which sample is drawn with the help of a blower. The CDP is mounted on a revolving swivel with a wing which always turns the inlet nozzle upwind. Right behind the nozzle is a laser beam (at 660 nm) which illuminates the cloud droplets entering the laser beam. The instrument classifies the droplets into size classes according to the amount of scattered light. Our CDP measures the droplet size distribution in the size range of 3–50 µm with 30 discrete size bins (3–14 µm with 1 µm bins and 16–50 µm with 2 µm bins) every 10 s. By knowing the sampling area (depth of field) of the laser beam (1.5 mm long, 200 µm thick) and the sample velocity at the nozzle (8.3–9.1 m s<sup>-1</sup> in our CDP), we are able to calculate cloud droplet concentrations at each bin and integrate them in order to get the total cloud droplet concentration. In order to lengthen its lifetime, the cloud droplet probe is switched off during summers, when the occurrence of cloud events is low, and during winters, when icing conditions take place.

### Weather camera

Our most recent installation at Puijo is a weather camera that is connected to a server (Axis 247S Video Server). The camera faces northward and supplies both a live-feed image and a still image every 15 minutes. We use the camera for visual check of the prevailing weather and for verifying the cloud events afterwards.

## Experimental setup at Savilahti

### Meteorological parameters

The automatic weather station (Vaisala Milos 500) at Savilahti includes instruments for measurement of temperature (Pentronic Pt100), relative humidity (Vaisala HMP45D), pressure (Vaisala PTB201A), present weather (Vaisala FD12P), wind speed and direction (Thies UA2D), cloud base height (Vaisala CT25K), rainfall (OTT Pluvio), snow depth (Campbell Scientific SR50–45), and sunshine duration (Siggelkow SONI). The instruments are located at the ground level (87 m a.s.l.), except the wind anemometer and the sunshine meter, which are located on the roof of the adjacent building approximately 15 and 10 m above the other instruments, respectively.

### Sun photometer

We measure aerosol optical properties also by using a sun photometer (Cimel 318A) that belongs to the AERONET network. Detailed description about these sun/sky measurements and the network is given by Holben *et al.* (1998). Measurements of the direct solar radiation provide information to retrieve the columnar aerosol optical depth (AOD), while the sky radiance measurements can be inverted to produce aerosol optical properties such as size distribution, single scattering albedo, phase functions, and the complex index of refraction. We carry out the direct sun measurements at wavelengths of 340, 380, 440, 675, 870, 940, and 1020 nm, and the sky radiance measurements at wavelengths of 440, 675, 870, and 1020 nm.

### Solar flux

We measure the global solar radiation with a pyranometer (CMP21) that belongs to the Sol-Rad-Net (Solar Radiation Network) network implemented as a companion to AERONET and also maintained by NASA. This pyranometer measures the global solar irradiance received at the horizontal surface in the spectral range from 310 nm to 2800 nm.

### Trajectory analysis

We used trajectory analysis to reveal the air mass arrival patterns, by calculating 120-hour backward trajectories for the years 2000–2006 in 3-hour intervals, by using FLEXTTRA trajectory model (Stohl *et al.* 1995). For classification, we split the whole set of 20 400 trajectories into five air mass arrival sectors, named as Arctic (315°–10°), Arctic/Kola (10°–70°), East (70°–160°), South (160°–235°) and Marine (235°–315°) (Fig. 1). The eastern and southern sectors represent the continental air/sources from Russia and Europe, respectively. The Marine sector covers the northern Atlantic and the two Arctic sectors the Arctic Ocean. We furthermore divided the Arctic sector into two sectors in order to separate the Kola Peninsula sources from the clean Arctic air. We classified each trajectory according to its main sector, i.e. the sector where it had spent most of the time during the last 120 hours.

## Results and discussion

### Atmospheric pressure

The hourly-average atmospheric pressure varied between 924 and 1016 hPa (average 974 hPa) during the three-year period from November 2005 to November 2008 at Puijo and between 949 and 1045 hPa (average 1000 mbar) at Savilahti (Table 3). The difference in the long-time average of atmospheric pressure between Puijo and Savilahti is 26 hPa which corresponds to the height difference of 219 m between the two stations, when air density of  $1.21 \text{ kg m}^{-3}$  is used. We could not find any annual variation in the atmospheric pressure.

### Temperature

The hourly-average temperature for the three-year period was between  $-28.5$  and  $27.2^\circ\text{C}$  (with an average of  $+3.4^\circ\text{C}$ ) at Puijo and between  $-35.8$  and  $29.7^\circ\text{C}$  (with an average of  $+4.4^\circ\text{C}$ ) at Savilahti (Table 3). We observed the lowest temperature at Puijo in January 2006 and at Savilahti in February 2007, and the high-

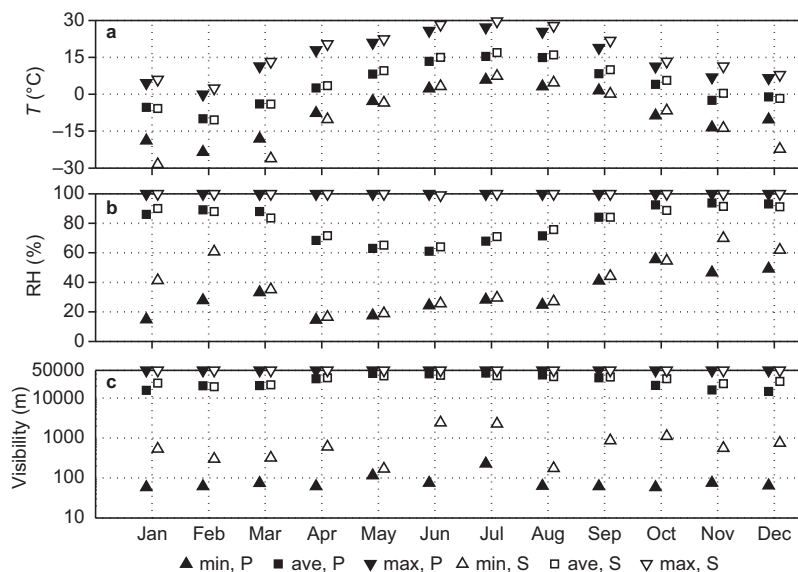


**Fig. 3.** (a) The monthly temperature, (b) relative humidity, and (c) visibility at Puijo (P) and Savilahti (S).

est temperatures both at Puijo and Savilahti in July 2006. We found that the difference between the monthly average temperatures at Puijo and Savilahti varied from month to month (Fig. 3a). Normally, the temperature at Savilahti is higher than at Puijo, but the opposite is true in the wintertime from December to March due to temperature inversion situations. The largest differences in the average monthly temperature between Savilahti and Puijo occurred in August

2008 ( $T_{\text{Savilahti}} - T_{\text{Puijo}} = +2.8^{\circ}\text{C}$ ) and in February 2007 ( $-2.2^{\circ}\text{C}$ ).

## Relative humidity

The statistics of the relative humidity was apparently the same for both the Puijo and Savilahti data (Table 3). We observed the highest relative humidity in winter and the lowest in summer

**Table 3.** Hourly minimum, 10th percentile, average, 90th percentile and maximum of the measured parameters at Puijo and Savilahti. Values below and above the measurement range are denoted with ‘less than’ and ‘more than’ symbols.

Component	Location	Min	10th percentile	Average	90th percentile	Max
Atmospheric pressure (hPa)	Puijo	924.0	958.7	973.7	989.6	1015.5
	Savilahti	949.3	984.6	999.7	1016.0	1044.5
Temperature (°C)	Puijo	-28.5	-8.4	3.4	15.9	27.2
	Savilahti	-35.8	-8.2	4.4	17.2	29.7
Relative humidity (%)	Puijo	15	47	80	100	100
	Savilahti	16	52	81	97	100
Visibility (m)	Puijo	55	230	28500	49560	> 50000
	Savilahti	170	5970	29590	> 50000	> 50000
Wind speed (m s <sup>-1</sup> )	Puijo	0.4	3.3	7.4	11.5	20.3
	Savilahti	< 0.1	1.3	2.7	4.4	9.1
Aerosol number concentration (cm <sup>-3</sup> )	Puijo	34	530	2040	3830	26260
Black carbon concentration (ng m <sup>-3</sup> )	Puijo	< 100	< 100	230	500	3540
Nitric oxide concentration (ppb)	Puijo	< 0.05	< 0.05	0.4	0.7	148
Nitrogen dioxide concentration (ppb)	Puijo	< 0.05	< 0.05	1.5	4.3	67
Ozone concentration (ppb)	Puijo	1.6	17	29	43	81
Sulphur dioxide concentration (ppb)	Puijo	< 0.1	< 0.1	1.2	2.2	144

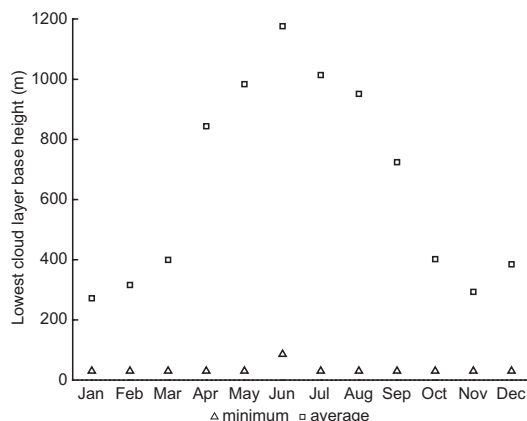


**Fig. 4.** The monthly height of the lowest cloud layer base at Savilahti.

months at both sites (Fig. 3b). In January and from April to August the relative humidity at Puijo was lower than at Savilahti. The opposite was true for the rest of the months when the tower is most often in cloud (Portin *et al.* 2009).

### Horizontal visibility

The average horizontal visibility was apparently the same at Puijo and Savilahti (Table 3). However, the minimum of the hourly averages of visibility values was 55 and 170 m at Puijo and

Savilahti, respectively. The average horizontal visibility was lower at Puijo from October to April (Fig. 3c), when also the majority of the cloud events occurred. During these months the 10th percentile of visibility values was below 200 m, which is one of our criteria for a cloud event (Portin *et al.* 2009). The monthly average of the cloud base height measured at Savilahti was below 400 m from October to March (Fig. 4), indicating frequent occurrence of low clouds during these months.

### Winds

We found that southerly to northwesterly (in clockwise direction) winds dominate at Puijo, as the compass points from SSE to NNW (clockwise) have the largest share (7%–9% each) in the wind distribution (Fig. 5a). The compass points from NNW to SSE (clockwise), excluding N to NNE, each have only a 4%–6% share. The sector from N to NNE has the lowest share, 2%. In order not to cause any confusion, we would like to point out that the wind directions given above are compass points from which the wind is blowing.

The hourly-average and maximum wind speed during the three-year period from November 2005 to November 2008 at Puijo were

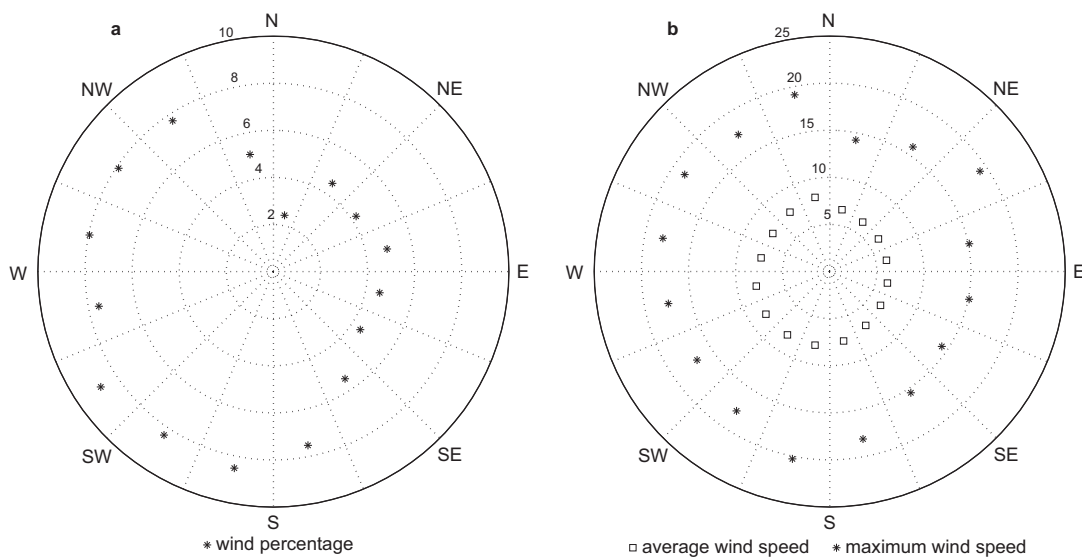


**Fig. 5.** (a) The wind percentage (%) and (b) the average and maximum wind speed ( $\text{m s}^{-1}$ ) at Puijo.

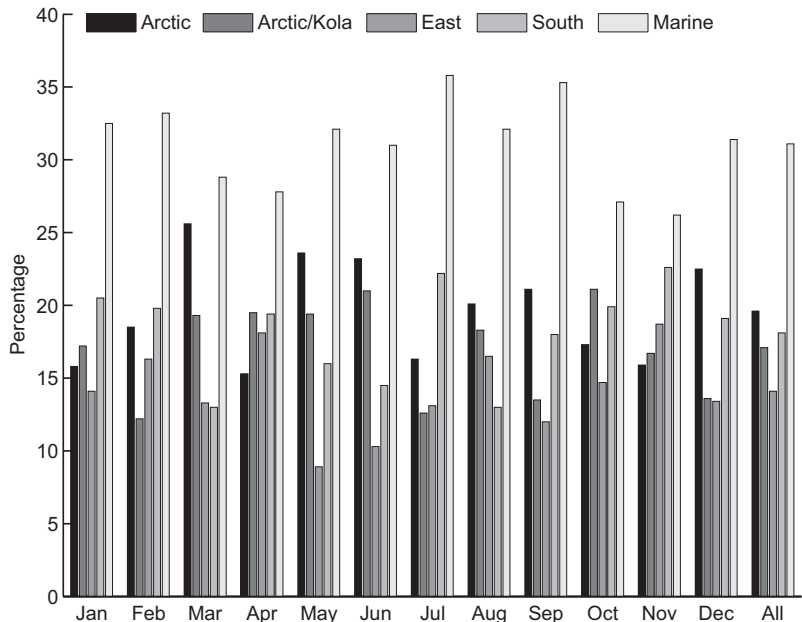


**Fig. 6.** The monthly percentages of times that the air masses arriving at Puijo have spent in each of the five sectors illustrated in Fig. 1.

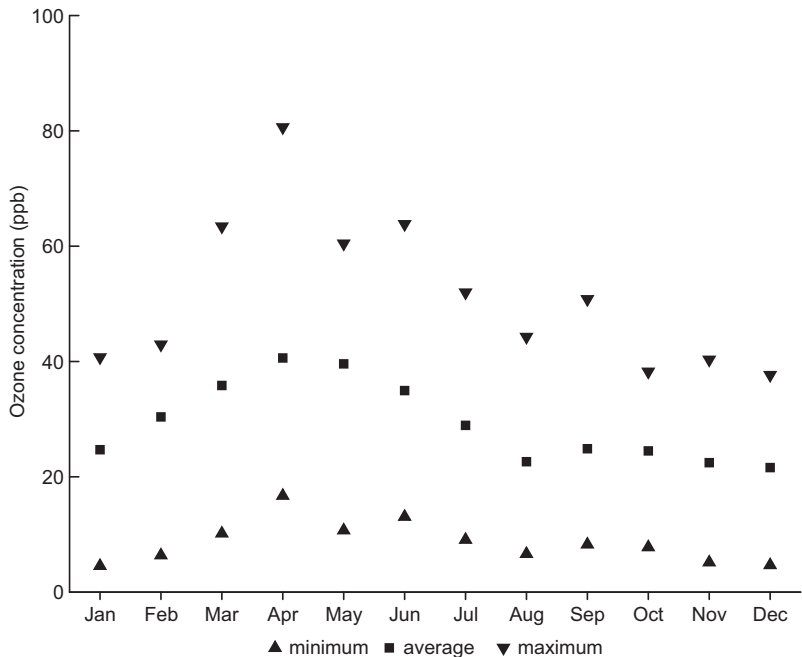


**Fig. 7.** The monthly ozone concentration at Puijo.

7.4 and 20.3 m s<sup>-1</sup>, respectively (Fig. 5b). We observed that the strongest winds were blowing from the south. At Savilahti the wind speed during the same period was 2.7 m s<sup>-1</sup> on an average and 9.1 m s<sup>-1</sup> at its maximum (Table 3). We can explain the remarkably lower wind speed at Savilahti by the fact that the Savilahti AWS station is surrounded by hills from each direction.

### Trajectory analysis

The trajectories were distributed relatively evenly throughout the year and we could not observe any clear seasonal pattern. In general, the two Arctic sectors altogether had about 37% and the Marine sector 31% of all trajectories (Fig. 6). It must be noted that since Puijo is located some hundreds

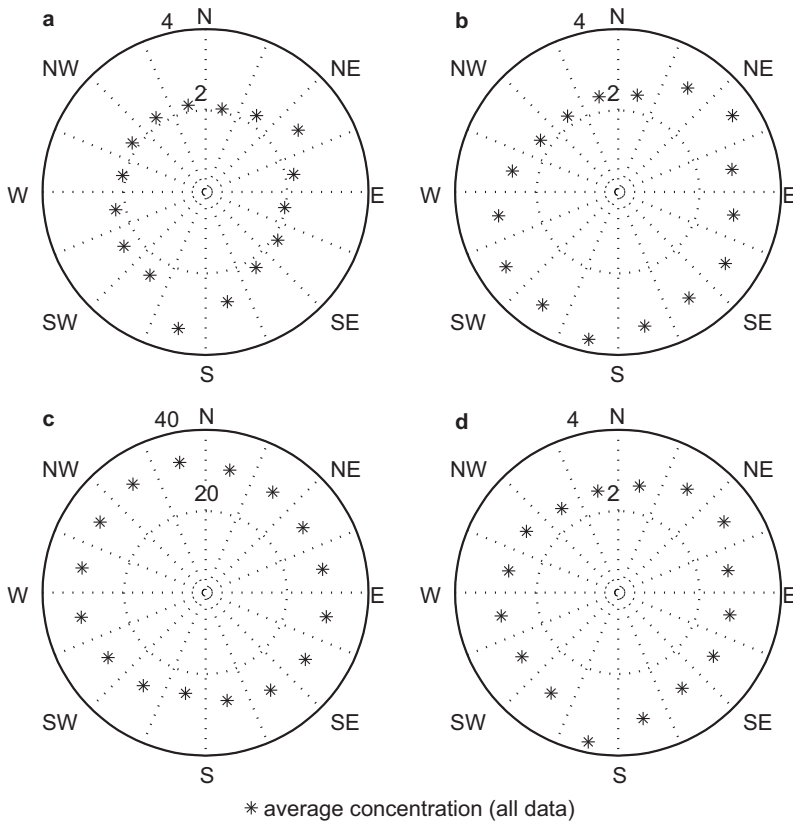


**Fig. 8.** The average concentration of (a) NO, (b) NO<sub>x</sub>, (c) O<sub>3</sub>, and (d) SO<sub>2</sub> at Puijo. In a, b, and d,  $\log(1000 \times C/\text{ppb})$ , where  $C$  is the measured concentration, is presented for clarity. In c the concentration unit is ppb.

of kilometers from the marine coastline (750 km—the closest distance to the Norwegian coastline), even the marine air masses have spent some time over land before arrival at Puijo. For Marine and Arctic air masses this time was on average 33 and 41 hours, respectively.

## Ozone

We analyzed the trace gas concentrations for the time period from November 2006 to November 2008. Besides the statistics (Table 3) we calculated the average and peak concentrations of the trace gases for 16 equally divided wind direction sectors (22.5° each). During the two-year time period the average ozone concentration was 29 ppb, varying between 1.6 and 81 ppb (Table 3). This is somewhat higher than the yearly average of ozone concentration at the ground level in Kuopio during years 1998–2006, which, according to the City of Kuopio officials, was 20–25 ppb ( $40\text{--}50 \mu\text{g m}^{-3}$ ).

We found that the ozone concentration at Puijo is highest in the spring (average in April 41 ppb) and lowest in the winter (average in November–December 22 ppb) (Fig. 7). The average of hourly ozone concentration at the ground level in Kuopio in 2006 was highest in the summer (average in May 70 ppb =  $140 \mu\text{g m}^{-3}$ ) and lowest in the winter (average in November 28 ppb =  $56 \mu\text{g m}^{-3}$ ).

We could not find any appreciable difference in ozone concentration with different wind directions when we inspected all the data at the same time (Fig. 8c). However, as ozone concentration is known to have a clear annual and daily cycle, and to depend on sunlight (e.g. Seinfeld and Pandis 2006), we calculated the deviation from a long-time (15 days) running average for ozone concentration as a function of wind direction for dark season (November to January) and light season (May to July) separately. We found that during the dark season the ozone concentration is lower when wind blows from the district heating plant (Fig. 9a). This is also the time when the

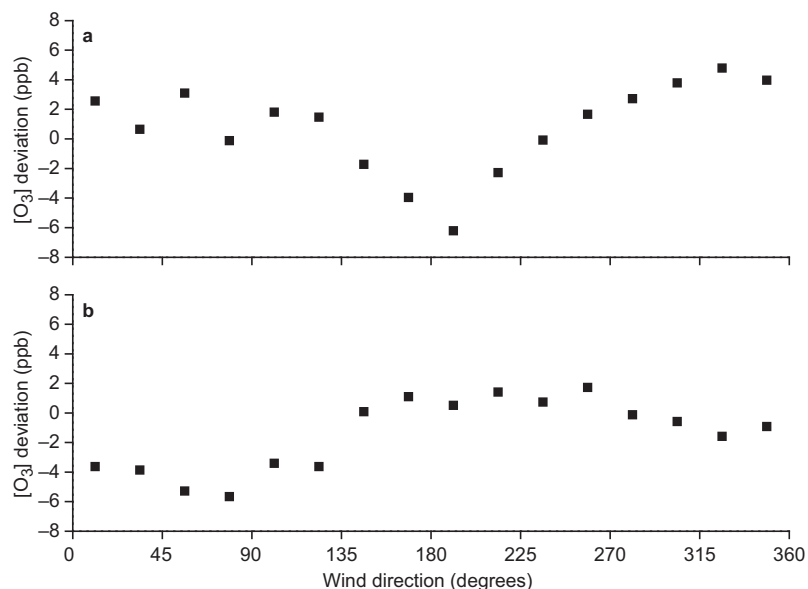


**Fig. 9.** The deviation of the measured ozone concentration from the 15-day moving average as a function of wind direction at Puijo for (a) dark season (from November to January) and for (b) light season (from May to July).

heating plant is operating near its full capacity and producing more pollutants, such as NO<sub>x</sub>, which destracts ozone. During the light season (Fig. 9b) the ozone concentration is reduced only when the wind blows from the northeastern sector where the pulp mill is located.

### Nitrogen oxides and sulphur dioxide

The long-time average of the hourly NO, NO<sub>2</sub> and SO<sub>2</sub> average concentrations at Puijo for the two-year period were 0.4, 1.5 and 1.2 ppb, respectively (Table 3). The concentration of NO, NO<sub>2</sub> and SO<sub>2</sub> was 23%, 12% and 6% of the time below the lower detection limit of their analyzers. We can explain the low NO concentration e.g. by the presence of ozone which reacts with NO. The maximum hourly average concentrations of NO, NO<sub>2</sub> and SO<sub>2</sub> we observed were 148, 67 and 144 ppb, respectively. The yearly average and maximum hourly average concentrations at the ground level in Kuopio in 2006 were 10 and 70 ppb for NO<sub>2</sub> (20 and 140  $\mu\text{g m}^{-3}$ ), and 0.7 and 25 ppb (2 and 67  $\mu\text{g m}^{-3}$ ) for SO<sub>2</sub>, respectively. Thus the NO<sub>2</sub> concentration is lower and SO<sub>2</sub> concentration higher at Puijo than at the ground level.

For both SO<sub>2</sub> and NO<sub>x</sub> (NO + NO<sub>2</sub>) the average wind direction dependent concentrations

were high when the wind was blowing either from northeast or from south (Fig. 8a, b, d). We can explain this dependence, at least partially, with the location of the pulp mill and the district heating plant, which lie roughly to the northeast and south from Puijo, respectively. In these sectors also the local traffic is intensive. We also suggest that the pulp mill and the district heating plant contribute to the SO<sub>2</sub> concentration at Puijo more than that at the ground level, as they release their emissions to approximately the same height where the Puijo measurement site is located.

### Aerosols

The long-time hourly average particle number concentration at Puijo during the time period from June 2006 to November 2008 was 2040  $\text{cm}^{-3}$  (range 34–26 260  $\text{cm}^{-3}$ ) (Table 3). For comparison, the long-time hourly average particle number concentrations were 700  $\text{cm}^{-3}$  at the Pallas background station (Komppula *et al.* 2003), and 2220  $\text{cm}^{-3}$  and 3210  $\text{cm}^{-3}$  in a boreal forest region in Hyttiälä and at a Baltic background station in Utö, respectively (Dal Maso *et al.* 2008).

The particle number concentration is highest in the spring and lowest in the autumn (Fig. 10a). The seasonal averages of the particle number

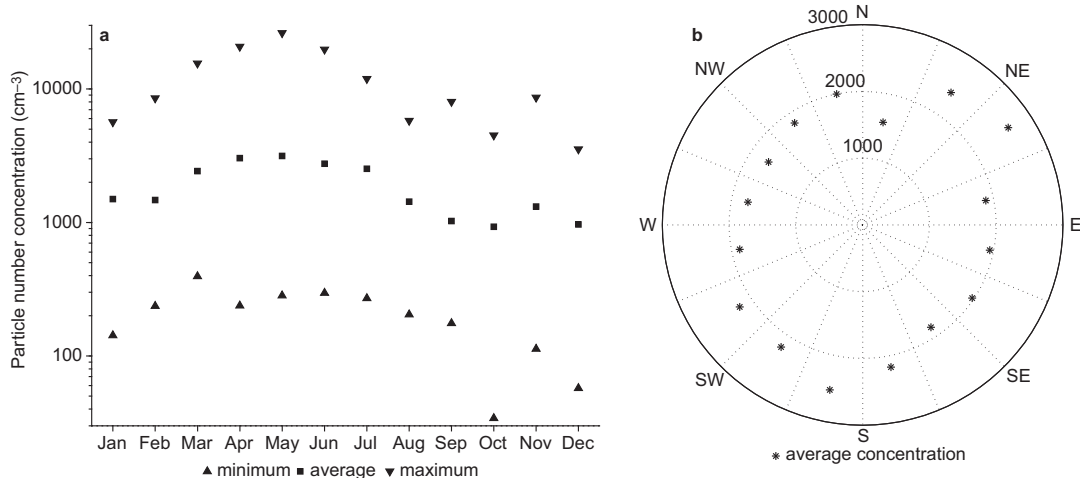


**Fig. 10.** The particle number concentration at Puijo (a) on a monthly basis and (b) as a function of wind direction. The concentration unit in b is cm<sup>-3</sup>.

concentration at Puijo are 2870, 2240, 1090 and 1310 cm<sup>-3</sup> in the spring (March–May), summer (June–August), autumn (September–November) and winter (December–February), respectively. At the Baltic Sea background station in Utö, the seasonal averages of the particle number concentration were 3315, 2789, 1830 and 1424 cm<sup>-3</sup> in the spring, summer, autumn and winter, respectively (Engler *et al.* 2007). The seasonal patterns are quite similar, excluding the wintertime, when the relative particle number concentration is higher at Puijo.

In the long-time average and its monthly distribution we have not separated cloud events with less unactivated submicron particles or rainy days from cloudless and clear days, since we measured these average number concentrations from the total air sampling line with a heated inlet. Otherwise, the cloud formation events, observed frequently in the autumn (Portin *et al.* 2009), would have decreased the average number concentration in the autumn even more.

At Puijo the long-time average concentration of Aitken (25–100 nm) and accumulation mode (100–800 nm) particles were 1100 and 470 cm<sup>-3</sup>, respectively. The particle concentration at Puijo is typical for a measurement site near an urban environment although lower than near the emission sources. For example, Tiitta *et al.* (2007) found that a long-time average concentration of ultrafine (3–100 nm) and accumulation mode

(100–900 nm) particles next to a road at Savilahti were 14 000 and 1600 cm<sup>-3</sup>, respectively. We did not investigate the nucleation mode (below 25 nm) particles at Puijo systematically in this paper, but we observed frequently new particle formation events, which tend to increase the nucleation mode particle concentration.

The above mentioned differences in aerosol number concentration also suggest that the fraction of the particles at Puijo emerging from local traffic may not be very high, or that the aerosol has been diluted and/or coagulated before reaching Puijo, since the measurement site is located over 200 m above the general street/highway level. However, we can see more clearly the influence of the pulp mill to the northeast and the district heating plant to the south of Puijo as an elevated particle number concentration when the wind blows from either of these two sources (Fig. 10b).

We found a clear dependence of the particulate black carbon concentration on wind direction (Fig. 11b). The BC concentration is highest with southwesterly winds (average BC concentration 390 ng m<sup>-3</sup>) and lowest with north-westerly winds (average BC concentration 100 ng m<sup>-3</sup>). The peak monthly average BC concentration occurred in March with a value of 410 ng m<sup>-3</sup> and the maximum hourly BC concentration in April 2008 with a value of 3530 ng m<sup>-3</sup>. The BC concentration was lowest in the summertime (Fig. 11a).

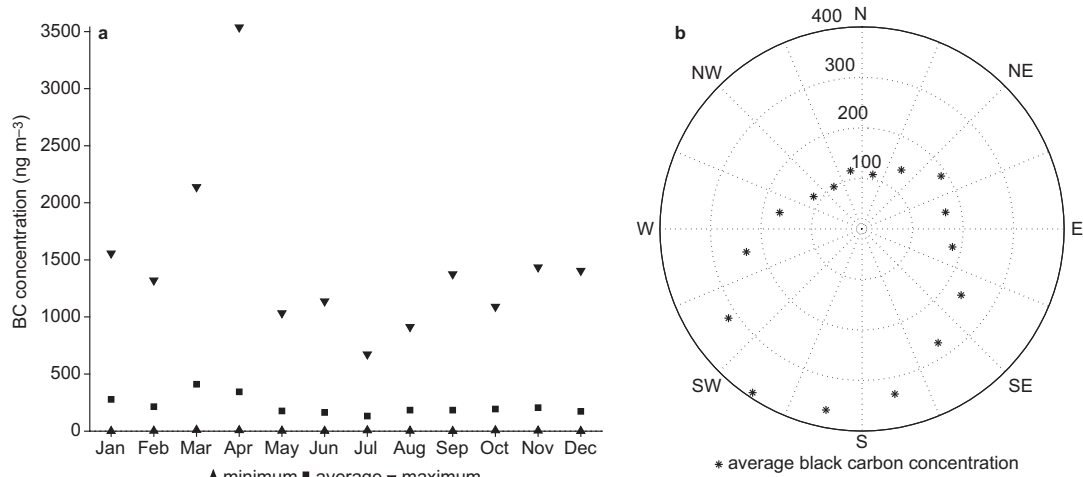


**Fig. 11.** The black carbon concentration at Puijo (a) on a monthly basis and (b) as a function of wind direction. The concentration unit in b is  $\text{ng m}^{-3}$ .

## Clouds

Here we present a summary of the occurrence of low-level clouds at Puijo and refer the reader to our other article for more details (Portin *et al.* 2009). We also give here some statistical figures concerning the clouds at Puijo.

We observed that the Puijo tower was approximately 160 times in cloud during the period between June 2006 and October 2008. These so called cloud events lasted from 15 minutes to 56.5 hours. Most of the events occurred in the autumn and early winter; e.g. in November the tower was inside a cloud 42% of the time, whereas the overall percentage for in-cloud situations was 10%. Icing conditions ( $T < 0^\circ\text{C}$ ) were observed throughout the winter.

The cloud droplet number concentration was highest in the autumn and lowest in the spring, being  $665 \text{ cm}^{-3}$  at its maximum and  $138 \text{ cm}^{-3}$  on the average. The average cloud droplet diameter ranged from  $3.2$  to  $16.6 \mu\text{m}$ .

## Summary

In the early 2000s, one of us (A. Laaksonen) noticed that the top of the Puijo tower is occasionally inside a cloud and supposed that the tower could be a possible place for cloud experiments. As the tower stands on a 150-m high hill,

it reaches altogether 230 m above the ground level. This enables also formation of orographic clouds when humid air rises up the steep side of the Puijo hill.

By looking at the cloud occurrence data, we can conclude that Puijo tower is a very good place to gather experimental data on cloud formation. The tower is also logically a brilliant place since the research staff from the University building can actually see with their own eyes when the tower is in cloud and we have an easy access to the tower.

Besides the high enough location, the surroundings are different in each side of the tower. There are distinct sectors for cleaner and more polluted air, which enables us to investigate the effect of local emission sources on aerosol and cloud properties at Puijo. In addition to the local sources, the trajectory calculation enables us to distinguish the properties of cleaner Arctic air masses from air masses coming from more polluted regions in east and south. In addition to cloud experiments, we can use the Puijo measurement station for studies of particle formation, which we also observed frequently.

Furthermore, comparison of long-time averages between Puijo and Pallas, a background measurement site, gives valuable, and so far unique information on the effect of urban aerosols on cloud formation, since such stationary measurement sites are rare worldwide.

**Acknowledgements:** The funding provided by the Academy of Finland Centre of Excellence program (project nos. 211483, 211484 and 1118615) is acknowledged. The authors acknowledge the financial support for instrumentation by the European Regional Development Fund (ERDF). The authors are very grateful for the technical support of A. Aarva, T. Anttila, A. Halm, H. Kärki, A. Poikonen and K. Ropponen from FMI's Observation Services.

## References

- Baltensperger U., Gäggeler H.W., Jost D.T., Lugauer M., Schwikowski M., Weingartner E. & Seibert P. 1997. Aerosol climatology at the high-alpine site Jungfraujoch, Switzerland. *J. Geophys. Res.* 102: 19707–19715.
- Dal Maso M., Hyvärinen A., Komppula M., Tunved P., Kerminen V.-M., Lihavainen H., Viisanen Y., Hansson H.-C. & Kulmala M. 2008. Annual and interannual variation in boreal forest aerosol particle number and volume concentration and their connection to particle formation. *Tellus* 60B: 495–508.
- Engler C., Lihavainen H., Komppula M., Kerminen V.-M., Kulmala M. & Viisanen Y. 2007. Continuous measurements of aerosol properties at the Baltic Sea. *Tellus* 59B: 728–741.
- Hatakka J., Aalto T., Aaltonen V., Aurela M., Hakola H., Komppula M., Laurila T., Lihavainen H., Paatero J., Salminen K. & Viisanen Y. 2003. Overview of the atmospheric research activities and results at Pallas GAW station. *Boreal Env. Res.* 8: 365–383.
- Holben B.N., Eck T.F., Slutsker I., Tanré D., Buis J.P., Setzer A., Vermote E., Reagan J.A., Kaufman Y., Nakajima T., Lavenu F., Jankowiak I. & Smirnov A. 1998. AERONET – a federated instrument network and data archive for aerosol characterization. *Remote Sens. Environ.* 66: 1–16.
- IPCC 2007. Summary for policymakers. In: *Climate change 2007: The physical science basis. Contribution of Working Group I to the Fourth Assessment Report of the Intergovernmental Panel on Climate Change*. Cambridge University Press, Cambridge.
- Komppula M., Lihavainen H., Hatakka J., Paatero J., Aalto P., Kulmala M. & Viisanen Y. 2003. Observations of new particle formation and size distributions at two different heights and surroundings in subarctic area in northern Finland. *J. Geophys. Res.* 108(D9), 4295, doi:10.1029/2002JD002939.
- Petzold A. & Schönlinner M. 2004. Multi-angle absorption photometry — a new method for the measurement of aerosol light absorption and atmospheric black carbon. *J. Aerosol Sci.* 35: 421–441.
- Portin, H. J., Komppula, M., Leskinen, A. P., Romakkaniemi, S., Laaksonen, A. & Lehtinen, K. E. J. 2009: Observations of aerosol–cloud interactions at the Puijo semi-urban measurement station. *Boreal Env. Res.* 14: 641–653.
- Seinfeld J. & Pandis S. 2006. *Atmospheric chemistry and physics. From air pollution to climate change*, 2nd ed. John Wiley & Sons, New York.
- Stohl A., Wotawa G., Seibert P. & Kromp-Kolb H. 1995. Interpolation errors in wind fields as a function of spatial and temporal resolution and their impact on different types of kinematic trajectories. *J. Appl. Meteorol.* 34: 2149–2165.
- Tiitta P., Miettinen P., Vaattovaara P., Laaksonen A., Joutsensaari J., Hirsikko A., Aalto P. & Kulmala M. 2007. Road-side measurements of aerosol and ion number size distributions: a comparison with remote site measurements. *Boreal Env. Res.* 12: 311–321.
- Weingartner E., Nyeki S. & Baltensperger U. 1999. Seasonal and diurnal variation of aerosol size distributions ( $10 < D < 750$  nm) at a high-alpine site (Jungfraujoch 3580 m asl). *J. Geophys. Res.* 104: 26809–26820.
- Wiedensohler A. 1988. An approximation of the bipolar charge-distribution for particles in the sub-micron size range. *J. Aerosol Sci.* 19: 387–389.